JACS Au
AN OPEN ACCESS JOURNAL OF THE AMERICAN CHEMICAL SOCIETY

pubs.acs.org/jacsau
Article

Development of an α-Klotho Recognizing High-Affinity Peptide Probe from In-Solution Enrichment

Peiyuan Zhang, Xiyun Ye, John C. K. Wang, Corey L. Smith, Silvino Sousa, Andrei Loas, Dan L. Eaton, Magdalena Preciado López,* and Bradley L. Pentelute*

Cite This: JACS Au 2024, 4, 1334−1344
Read Online
ACCESS | Metrics & More | Article Recommendations | Supporting Information

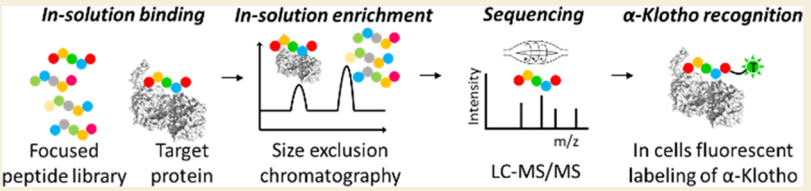

ABSTRACT: The kidney, parathyroid gland, and choroid plexus express the aging-related transmembrane protein α-Klotho, a coreceptor of the fibroblast growth factor 23 (FGF23) receptor complex. Reduced α-Klotho levels are correlated with chronic kidney disease and other age-related diseases, wherein they are released from membranes into circulation. Klotho's potential physiological action as a hormone is of current scientific interest. Part of the challenges associated with advancing these studies, however, has been the long-standing difficulty in detecting soluble α-Klotho in biofluids. Here, we describe the discovery of peptides that recognize α-Klotho with high affinity and selectivity by applying in-solution size-exclusion-based affinity selection-mass spectrometry (AS-MS). After two rounds of AS-MS and subsequent N-terminal modifications, the peptides improved their binding affinity to α-Klotho by approximately 2300-fold compared to the reported starting peptide Pep-10, previously designed based on the C-terminal region of FGF23. The lead peptide binders were shown to enrich α-Klotho from cell lysates and to label α-Klotho in kidney cells. Our results further support the utility of in-solution, label-free AS-MS protocols to discover peptide-based binders to target proteins of interest with high affinity and selectivity, resulting in functional probes for biological studies.

KEYWORDS: *α-Klotho, FGF23, affinity selection-mass spectrometry, peptide modifications, affinity enrichment, fluorescence imaging*

1. INTRODUCTION

α-Klotho (hereinafter abbreviated as Klotho) is a transmembrane protein related to aging.[1,2] Klotho acts as a coreceptor for fibroblast growth factor 23 (FGF23) by binding to fibroblast growth factor receptors (FGFR) 1c, 2c, and 4, to primarily regulate phosphate homeostasis in the kidney.[3−6] When the extracellular domain of Klotho is cleaved by the ADAM family proteases, it is secreted into circulation as soluble Klotho.[4] Klotho levels significantly decrease in various age-related dysfunctions, including diabetes, cancers, Alzheimer's disease, and chronic kidney disease (CKD).[6−9] In support of potential clinical relevance, it was shown that a single administration of low-dose secreted Klotho (10 μg/kg) was able to enhance memory in aging rhesus macaques.[10] In addition, Klotho is thought to have an antifibrotic effect in CKD.[8,11] Given its role as a biomarker and a potential hormone, it is crucial to develop reagents capable of accurately detecting Klotho with high affinity and selectivity. Availability of Klotho-selective probes will aid in the early detection of aging-associated diseases and facilitate the development of antiaging therapies.

Although antibodies are available for mouse and human Klotho, there is a lack of tools to detect Klotho in its native conformation in biofluids and tissues. Compared with macromolecules such as antibodies, peptides have advantageous biodistribution profiles, characterized by higher uptake and better permeability in tissues and more rapid clearance from serum, and as such it is desirable to develop peptide-based Klotho-selective probes. Recent structural studies of the FGFR/Klotho/FGF23 ternary complex have inspired the scientific community to investigate the interaction between FGF23 and Klotho (Figure 1A).[4] Peptides can mimic the multivalent and cooperative binding interfaces between two proteins, making them a valuable tool in targeting protein−protein interactions (PPIs).[12] The Dimarchi group successfully utilized the C-terminus of FGF23, which engages Klotho, to develop an FGF23 C-terminus mimicking peptide known as Pep-10 (Figure 1B).[13] Pep-10 demonstrated an antagonizing effect on FGF23 signaling in cells, showcasing the successful

Received: October 23, 2023
Revised: February 22, 2024
Accepted: February 23, 2024
Published: April 10, 2024

https://doi.org/10.1021/jacsau.3c00650
JACS Au 2024, 4, 1334−1344

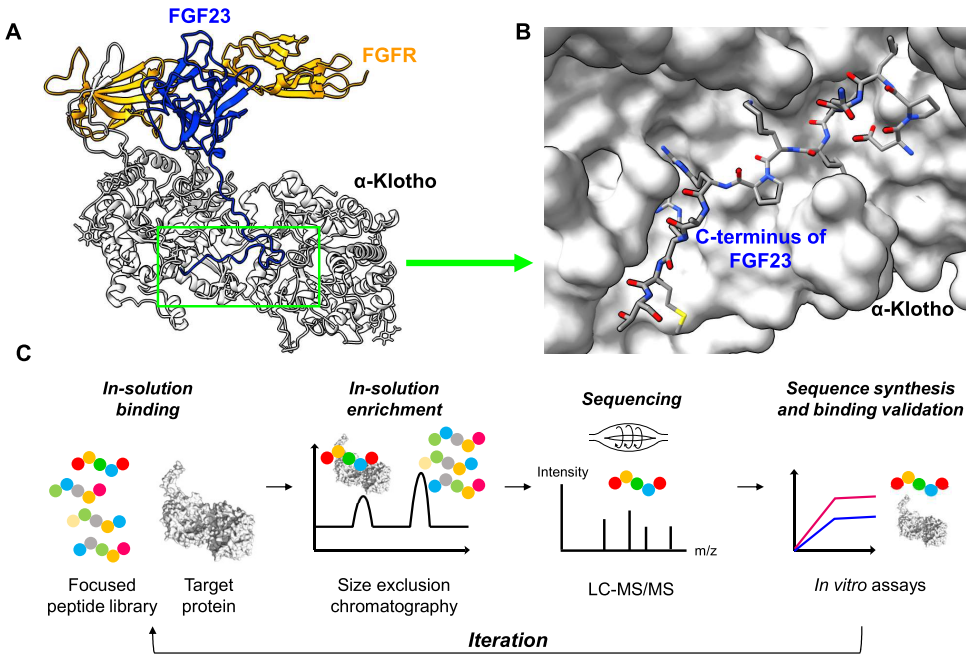

Figure 1. AS-MS enables in-solution enrichment and sequencing of high-affinity peptides based on the C-terminus of FGF23. (A) Structure of the protein−protein interaction between coreceptor protein Klotho, receptor protein FGFR, and signaling protein FGF23, modified from PDB: 5W21. Klotho is in white, FGFR protein is in yellow, and FGF23 is in blue. (B) Visualization of the binding pocket of Klotho and the C-terminus of FGF23. $FGF23^{188-200}$ is shown as sticks and the Klotho van der Waals protein surface is shown in white. (C) Schematic flowchart of AS-MS platform including in-solution binding and enrichment, sequencing, peptide sequence synthesis, and binding validation.

design of peptides based on PPIs involving Klotho. However, Pep-10 only had micromolar binding affinity toward Klotho. Based on the work referenced above, we developed a series of branched peptides to target Klotho with 100-fold enhanced affinity relative to Pep-10 using automated fast-flow synthesis.[14] Despite their enhanced performance, multimeric peptides have only modest binding affinity (10−100 nM) and a high molecular weight (>4 kDa) compared to traditional small molecules, potentially limiting their future applications in biological systems.

To increase binding affinity while decreasing molecular weight, we performed affinity maturation on the monomeric peptide Pep-10 via affinity selection-mass spectrometry (AS-MS) and rational design using our recently established in-solution enrichment platform for target-based high-affinity peptide binder discovery.[15] We discovered a monomeric peptide reagent named K18 with ∼2300-fold increased binding affinity toward Klotho compared to Pep-10 while keeping its molecular weight to ∼1.8 kDa. Based on our findings, we envision K18 as a versatile tool for further development of variants to investigate soluble and membrane-bound Klotho in biological milieu.

2. RESULTS AND DISCUSSION

2.1. Rational Design Identified Preliminary High-Affinity Peptides Targeting Klotho

Prior sequence mapping of the binding domain of FGF23 with Klotho unveiled the top-performing peptide Pep-10 (Figure S1; sequence: PMASDPLGVVRPRARM), which was selected by us as a lead scaffold for further optimization by affinity maturation.[13] The binding affinity of Pep-10 to recombinant mouse α-Klotho (mKlotho) was measured by biolayer interferometry (BLI). In the direct binding measurements by BLI, Pep-10-Biotin was immobilized on streptavidin tips, and serial dilutions of mKlotho were incubated with the tips to evaluate association and dissociation rates against Pep-10-Biotin. The direct dissociation constant (K_D) of the Pep-10/mKlotho interaction was determined in this manner to be 2.3 ± 0.5 μM.[14] In a competition BLI binding assay where in-solution Pep-10 competes against immobilized Pep-10-Biotin for mKlotho binding, we can assess competition K_D values and confirm Klotho site-specific binding.[16] In brief, Pep-10-Biotin was immobilized onto the streptavidin biosensor tips. Increasing concentrations of unlabeled Pep-10 were incubated with a constant concentration of mKlotho (100 nM) until equilibrium was reached. Pep-10-Biotin immobilized tips were then immersed into these solutions, and the binding events observed were used to estimate the fraction of unbound mKlotho to interpolate the competition K_D value. Pep-10 gave a competition K_D value of 5.9 ± 1.1 μM (Figure S2).

Terminal modifications of peptide binders with small molecules have the potential to alter peptides' binding affinity and kinetics to their protein targets. A tryptophan addition at the C-terminus of an MDM2-binding peptide has been shown to enhance binding by 50-fold by engaging a secondary binding pocket.[17] In another report, fluorescein addition at the N-terminus improved peptide binding to replication protein A by 1000-fold.[18] Recently, terminal modifications on an E6AP-derived, LXXLL motif-containing peptide improved its binding to the HPV-16E6 protein by more than 600-fold.[19] In this work, we serendipitously observed an increased binding affinity with the N-terminal attachment of fluorene onto Pep-10. The resulting peptide K1 (Figure S1; sequence: fluorenyl-PMASDPLGVVRPRARM) rendered a competition K_D = 66 ± 28 nM, which is 89-fold higher compared to Pep-10 in BLI competition binding assays using Pep-10-Biotin (Figure S2). We then performed alanine scanning on K1 to determine the residues that are critical for binding. We also investigated if this

https://doi.org/10.1021/jacsau.3c00650
JACS Au 2024, 4, 1334−1344

A

Name	N-term	Sequence	ALC%	Comp. K_D, nM
Pep-10	-	P M A S D P L G V V R P R A R M	-	5906 ± 1073
K1	Fluorenyl	P M A S D P L G V V R P R A R M	-	66 ± 28
K2	Fluorenyl	- M A S D P L G V V R P R A R -	-	56 ± 20
K3	Fluorenyl	- - A S D P L G V V R P R A R -	-	64 ± 27
K4	Fluorenyl	- - A S D P L G V V R P R A - -	96	139 ± 43
K5	Fluorenyl	- - A S D P L G V V R P R - - -	-	357 ± 66
K6	Fluorenyl	- - A S D P L G V V K A R A - -	92	66 ± 19
K7	Fluorenyl	- - A S D P L G V V K V R A - -	97	132 ± 39
K8	Fluorenyl	- - A S E P L G V V n Q R A - -	94	138 ± 37
K9	Fluorenyl	- - A S D P L G V V K Q R A - -	93	80 ± 25
K10	Fluorenyl	- - A S D P L G V V n Q R A - -	94	134 ± 22
K11	Fluorenyl	- - A S D P L G V V K N R A - -	92	63 ± 18
K12	**Fluorenyl**	**- - A S D P L G V V R G R A - -**	**96**	**19 ± 13**
K13	Fluorenyl	- - A S D P L G V V R A R A - -	96	24 ± 11
K14	Fluorenyl	- - A S D P L G V V n E R A - -	94	117 ± 47
K15	Fluorenyl	- - A S D P L G V V R Q R A - -	93	64 ± 20
K16	Fluorenyl	- - A S D P L G V V R e R A - -	92	108 ± 21
K17	Fluorenyl	- - A S D P L G V V R G R A R -	-	9 ± 5
K17′	Fluorenyl	- - A S D P L G V V R G R A R - *n*	-	10 ± 6

B

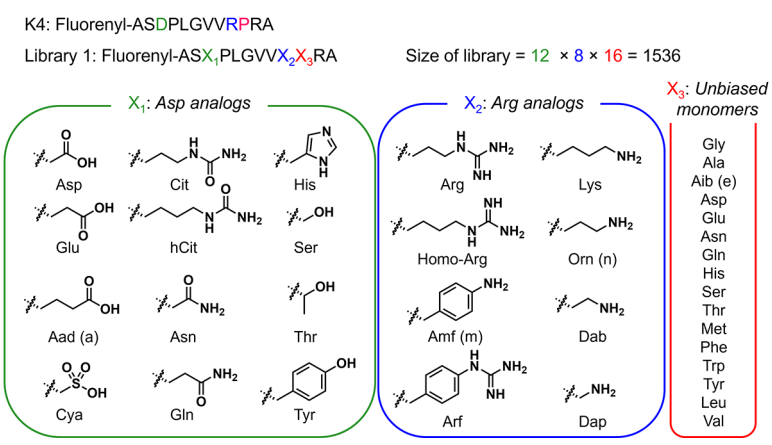

Figure 2. First round of AS-MS discovers K12 as a high-affinity peptide targeting Klotho from focused Library 1. (A) Sequence table of peptides targeting Klotho. Pep-10 is the initially reported peptide. K1−K5 are peptides in truncation studies that enable affinity selection and sequencing. K6 to K16 are peptides selected from the first round of AS-MS. K17 and K17′ are modified peptides based on the top-performing sequence K12. Average local confidence (ALC) score is an indicator of the sequencing confidence. In this table, "n" represents L-ornithine, "e" represents 2-aminoisobutyric acid, "*n*" represents D-ornithine, "Comp. K_D" represents competition K_D. Values represent the mean ± SD. All assays were run in two biological replicates. (B) Design of a 1536-member focused Library 1 based on K4. Abbreviations: Cit, citrulline; hCit, homocitrulline; Aad (a), aminoadipic acid; Cya, cysteic acid; Orn (n), L-ornithine; Amf (m), 4-amino-phenylalanine; Dab, 2,4-diaminobutyric acid; Arf, 4-guanidino-phenylalanine; Dap, 2,3-diaminopropionic acid; Aib (e), 2-aminoisobutyric acid.

enhanced binding observed on K1 by attachment of fluorene is due to nonspecific binding to Klotho.[16] Sixteen single alanine variants of peptide K1 were synthesized (Figure S1), namely, K-AS-1 to K-AS-16. Their competition K_Ds were determined by BLI (Figure S3). Alanine scanning identified hotspot residues Asp5, Pro6, and Arg11 because their respective Ala variants, D5A, P6A, and R11A, demonstrated a much lower ability to compete off Pep-10 for mKlotho binding (Figure S3). These Ala variants displayed abrogated binding to mKlotho, even upon fluorenyl modification, demonstrating that the binding of K1 to Klotho is sequence-dependent and not promiscuous due to the fluorene group. Notably, we discovered a higher affinity variant by substituting Pro12 in K1 to Ala, decreasing the competition K_D to 15 nM, a 5-fold higher affinity value than K1 (Figure S3).

2.2. Peptide Truncation Enabled Affinity Selection and Sequencing of Peptide Binders

AS-MS is a high-throughput technique to enable rapid screening of small molecule and peptide libraries.[20,21] Because the molecules of interest are self-encoded by their own unique mass, they do not need to be tagged and can thus be tested in mixtures against protein targets. Recently, we established an in-solution enrichment platform to screen peptide libraries based on high-performance size exclusion chromatography (HPSEC) coupled with liquid chromatography-tandem mass spectrometry (HPSEC−LC−MS/MS).[15] Briefly, using the split-and-pool solid-phase synthesis method, "focused" peptide libraries are prepared by randomizing select residues within the sequence of a known peptide binder. The libraries are incubated with a protein target in solution with different peptide:protein ratios. The mixture is then subjected to HPSEC to enrich peptide binders from the library bound to the protein target. The protein fraction that contains bound peptides is processed and decoded in an Orbitrap LC−MS/

https://doi.org/10.1021/jacsau.3c00650
JACS Au 2024, 4, 1334−1344

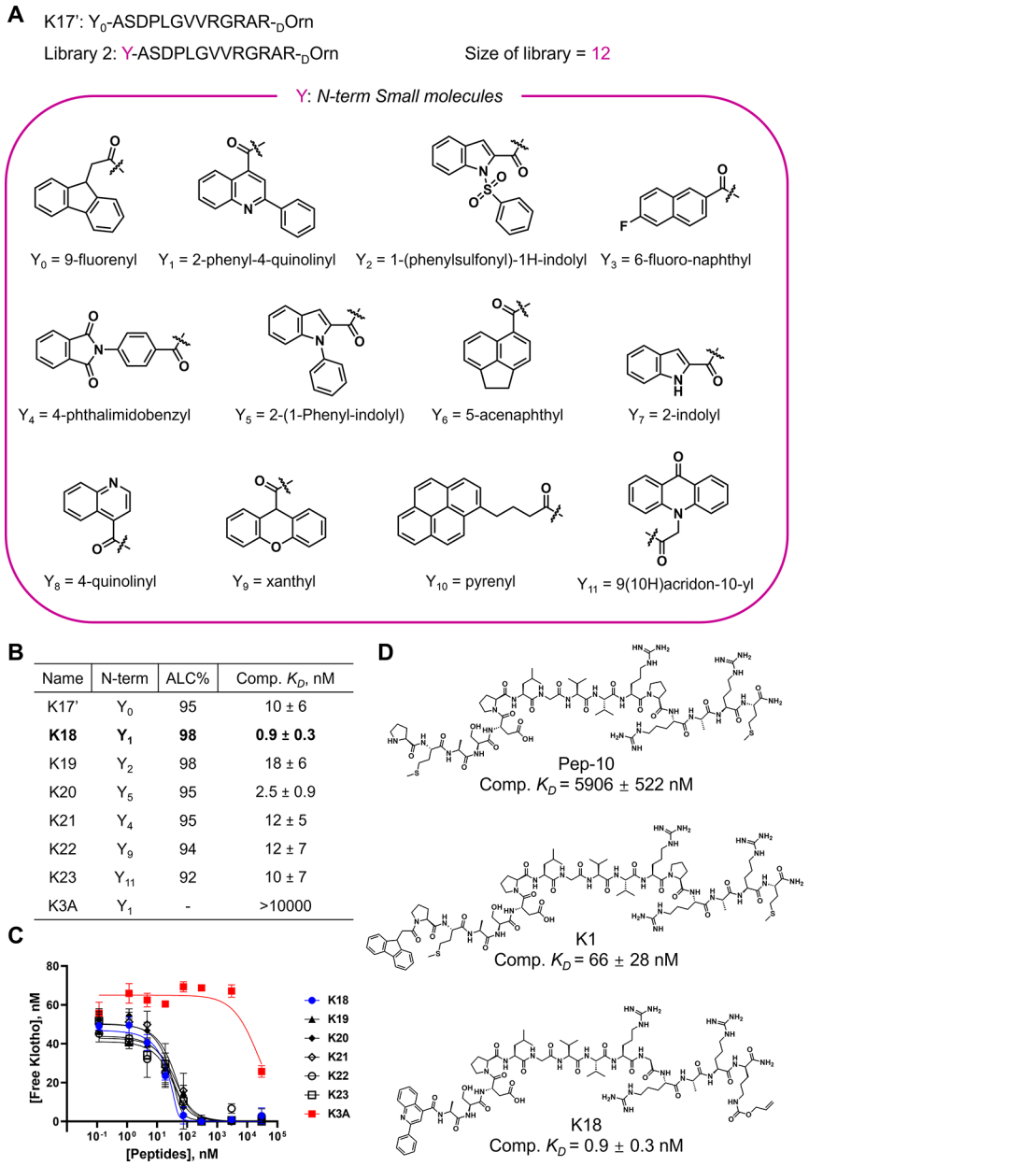

Name	N-term	ALC%	Comp. K_D, nM
K17′	Y_0	95	10 ± 6
K18	**Y_1**	**98**	**0.9 ± 0.3**
K19	Y_2	98	18 ± 6
K20	Y_5	95	2.5 ± 0.9
K21	Y_4	95	12 ± 5
K22	Y_9	94	12 ± 7
K23	Y_{11}	92	10 ± 7
K3A	Y_1	-	>10000

Figure 3. Second round of AS-MS discovers K18 as a high-affinity peptide targeting Klotho from focused Library 2. (A) Design of a 12-member focused Library 2 based on K17′. (B) Table of peptides targeting Klotho. K17′ has the initial N-term fluorene small molecule. K18 to K23 are peptides selected from the second round of AS-MS. K3A is the D5A/P6A/R11A triple variant peptide used as a negative control. (C) Representative binding curves of the competition binding assay with BLI-determined competition K_Ds in panel B. All assays were run in two biological replicates. (D) Chemical structures of Pep-10, K1 and K18. "Comp. K_D" represents competition K_D. Values represent the mean ± SD.

MS instrument. The decoded sequences are resynthesized and validated by biochemical and physical assays (Figure 1C).

The 16-mer long K1 reduced sequencing efficiency and accuracy in LC−MS/MS.[21,22] Additionally, three Arg residues close to the C-terminus of K1 can act as charge traps, resulting in incomplete fragmentation that impedes sequencing.[23] Therefore, we performed peptide truncation on K1 to facilitate downstream AS-MS selections. In a stepwise fashion, we truncated N- or C-terminal residues from K1, while keeping fluorene installed at the N-terminus. Pro1, Met2, and Met16 did not affect binding affinity to mKlotho as K2 and K3 have competition K_Ds of 56 ± 20 and 64 ± 27 nM, respectively, similar to K1. Arg15 and Ala14 are important for binding since the competition K_D values for K4 and K5 significantly increase (Figures 2A and S1).

K3 was not chosen as the parent peptide because it has three discrete Arg residues, resulting in poor sequencing by LC−MS/MS. K5 was not used further because of the decreased binding affinity relative to K1 determined by BLI experiments (K_D = 357 ± 66 nM). We chose K4 (Figure S1; sequence: fluorenyl-ASDPLGVVRPRA) as the parent peptide for affinity maturation since it is a 12-mer with two Arg residues while retaining relatively high binding affinity to Klotho with a competition K_D of 139 ± 43 nM (Figure S2). Pilot experiments with K4 were performed to ensure that it can be enriched in the Klotho protein fraction by HPSEC. 50 μg of mKlotho was incubated with 50 ng of K4 and subjected to

https://doi.org/10.1021/jacsau.3c00650
JACS Au 2024, 4, 1334−1344

HPSEC. LC−MS analysis showed no overlap between the K4 and protein fractions, indicating complete separation of the protein target from K4 (Figure S4A). The eluted fraction corresponding to mKlotho was subsequently analyzed by LC−MS/MS to confirm the recovery of K4. Its recovery yield, defined as the amount of peptide detected in the eluted Klotho fraction divided by the total amount of peptide before being mixed with Klotho, was 0.5%, which is above the threshold of 0.1% for AS-MS.[15] The sequencing average local confidence (ALC) score, an indicator of sequencing confidence, was 96%, which is above the threshold of 90%, indicating the accurate sequence assignment of K4 (Figure 2A).

2.3. AS-MS Discovers High-Affinity Peptides Targeting Klotho

To benchmark our AS-MS approach, focused Library 1 (Figure 2B; sequence: Fluorenyl-ASX_1PLGVVX_2X_3RA, where X is randomized residue) based on K4 was prepared. Two hotspots, Asp (X_1) and Arg (X_2) were mutated to analogs of Asp and Arg, respectively. The Pro residue (X_3) was mutated to an unbiased set of monomers, as its mutation to Ala improves binding affinity by five-fold. The focused library contains 1536 distinct members (Figure 2B). Library 1 was incubated with 50 μg of mKlotho, separated through HPSEC, and decoded by LC−MS/MS. The elution time of Library 1 did not overlap with the protein elution time, indicating complete separation of the protein target from the library (Figure S4B). In total 37 peptide sequences were identified with ALC scores >70% (Table S1). Eleven sequences numbered K6−K16 were selected and resynthesized due to their high ALC scores (≥92%) for validation in competition binding assays with BLI (Figures 2A and S4). Five out of 11 peptides gave competition K_D values at least two-fold lower than the parent peptide K4 (competition K_D < 70 nM). The top-performing sequence K12 (Figure S1; sequence: fluorenyl-ASDPLGVVRGRA) containing a single P to G mutation emerged as the highest binding affinity peptide, with a competition K_D of 19 ± 13 nM, which is seven-fold higher than K4 (Figure S5). Learning from the truncation study, we added back the Arg at the C-terminus and achieved K17 (Figure S1; sequence: fluorenyl-ASDPLGVVRGRAR) with a competition K_D of 9 ± 5 nM (Figure S6). An Alloc-protected $_D$Orn for late-stage modification was introduced onto K17 to provide K17′. This modification had no effect on binding as K17′ has a competition K_D of 10 ± 6 nM (Figure S6).

To further investigate the binding enhancement of N-terminal modifications, we replaced the N-terminal fluorene of K17′ with a small molecule chemical library to prepare focused Library 2 containing 12 distinct members (Figure 3A, sequence: Y-ASDPLGVVRGRAR-$_D$Orn, where Y is a randomized small molecule). Library 2 again went through the AS-MS process (Figure S4B). In total, ten peptide sequences were enriched (Table S2). Six sequences denoted as K18 to K23 (ALC scores ≥90%) were selected and resynthesized for validation in competition binding assays with BLI (Figure 3B,C). Generally, heterocyclic small molecules at the N-terminus improved the binding affinity. The sequence of K18 with N-terminal 2-phenyl-4-quinoline (Y_1) (Figure 3D; sequence: Y_1-ASDPLGVVRGRAR-$_D$Orn) emerged as the highest binding affinity peptide with a competition K_D value of 0.9 ± 0.3 nM (Figure 3C). Competition K_D of K18 is 73-fold higher than that of the parent peptide K1 and 6600-fold higher than that of the initially reported peptide Pep-10 (Figure 3D). Alanine scanning identified three hotspot residues to be critical for binding. Therefore, the D5A/P6A/R11A triple variant peptide K3A (Figure S1; sequence: Y_1-ASAALGVVAPRAR-$_D$Orn) with competition K_D > 10 μM was used as a negative-control peptide in this work (Figure 3C).

Biotinylated K18 and K3A were prepared as K18-Biotin and K3A-Biotin (Figure S1). K18-Biotin has a K_D of 1.0 ± 0.3 nM against mKlotho in the direct binding measurements by BLI, which is 2300-fold higher than that of the initially reported peptide Pep-10, while K3A-Biotin has no detectable binding by BLI (Figure S7). K18-Biotin's binding selectivity was also evaluated toward two additional proteins, MDM2 and 12CA5. In the direct binding measurements by BLI, K18-Biotin had no binding to these two proteins, indicating K18's binding to Klotho is selective (Figure S8).

The K18 and K3A peptides were labeled with the fluorophore 5-carboxytetramethylrhodamine (TAMRA) to obtain K18-TAMRA and K3A-TAMRA (Figure S1). We determined their apparent dissociation constants K_D to be 3.5 ± 1.4 nM and >10 μM, respectively, estimated by a fluorescence polarization assay (Figure S9). This orthogonal assay suggested fluorophore-labeled K18 retains a nanomolar binding affinity to Klotho. K18-TAMRA and K3A-TAMRA were then evaluated in the competition binding assays with BLI to compare with unlabeled molecules. The competition K_D of K18-TAMRA was determined as 1.3 ± 0.4 nM (Figure S10), which is similar to K18 (competition K_D = 0.9 ± 0.3 nM). We observed minimal K3A-TAMRA binding to Klotho (competition K_D > 10 μM). In summary, these findings suggest that the binding between K18 and mKlotho is not affected by TAMRA modification.

Mouse α-Klotho (accession number: O35082) and human α-Klotho (hKlotho, accession number: Q9UEF7) share 87% sequence identity and 92% similarity (the number of residues that are either identical or have similar chemical properties) calculated by Protein BLAST.[24] Residues of hKlotho interacting with the C-terminus of FGF23 (PDB: 5W21) are more conserved, with 98% similarity to mKlotho. We measured the direct binding of K18-Biotin to hKlotho by BLI (Figure S11). The experimentally determined K_D was 1.5 ± 0.6 nM, comparable to the K_D of K18-Biotin binding to mKlotho (K_D = 1.0 ± 0.3 nM). In the competition binding assay with BLI, K18 bound hKlotho with competition K_D = 1.2 ± 0.4 nM (Figure S12), similar to the competition K_D of K18 against mKlotho (0.9 ± 0.3 nM). The negative control peptide K3A returned a K_D > 10 μM to hKlotho as expected (Figure S12). These results demonstrated that K18 could be employed for further development as an affinity reagent to target not only mKlotho but also hKlotho. K18-TAMRA displayed competition K_D = 1.6 ± 0.4 nM to hKlotho while K3A-TAMRA returned a K_D > 10 μM, indicating that the binding affinity of K18 to hKlotho is not affected by TAMRA modification (Figure S12).

These biophysical assays demonstrated that, after two rounds of AS-MS, K18 was selected with a significantly enhanced binding affinity toward Klotho compared to the initially reported peptide Pep-10 without increasing molecular weight. Pep-10 shows a direct K_D of 2.3 μM in the direct binding measurements and a competition K_D of 5.9 μM in the competition binding assays. K18 has a direct K_D of 1.0 nM, which is 2300-fold lower than that of Pep-10 in the direct binding measurements and a competition K_D of 0.9 nM, which is 6600-fold lower than that of Pep-10 in the competition

https://doi.org/10.1021/jacsau.3c00650
JACS Au 2024, 4, 1334−1344

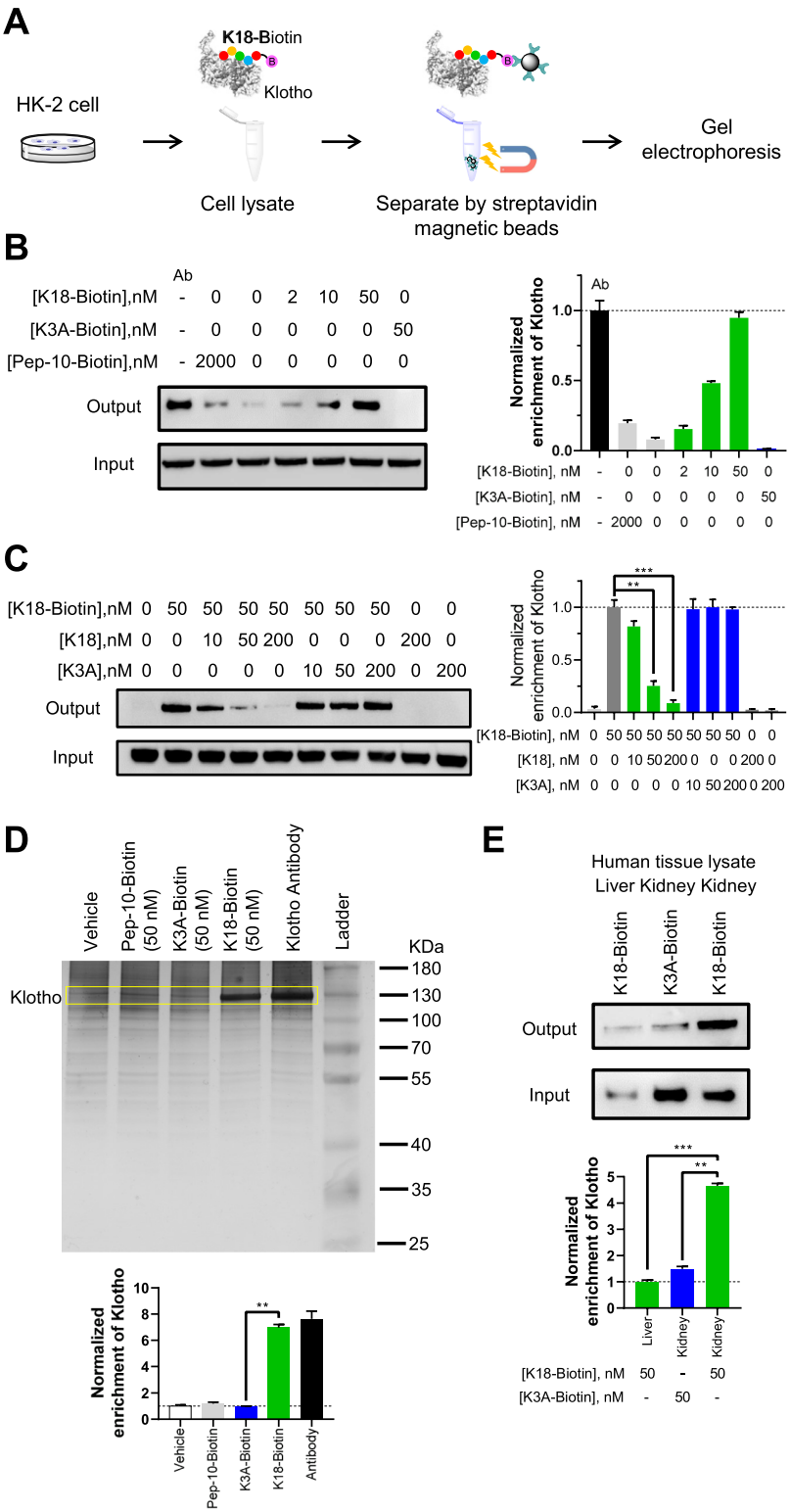

Figure 4. Pull-down assays show direct Klotho engagement by K18. (A) Schematic representation of pull-down assay workflow. K18-Biotin was incubated with HK-2 cell lysate and pulled down by streptavidin magnetic beads (Dynabeads MyOne Streptavidin T1). K18-Biotin-bound proteins were released and separated by gel. (B) Pull-down probe K18-Biotin enriched endogenous hKlotho from HK-2 cell lysate in a dose-dependent manner. Negative-control probe K3A-Biotin displayed no enrichment of Klotho at 50 nM. Pep-10-Biotin moderately enriched Klotho at 2 μM. The pull-down fraction at the first lane was generated by Klotho antibody (Ab) incubated with HK-2 cell lysate then pulled down by Dynabeads Sheep Anti-Rat IgG. Klotho antibody-bound proteins were then released and separated on gel with other samples. "Input" or "Output" western blots were performed on protein samples before or after pull-down. Before pull-down, 20% of total protein from cell lysate sample was prepared and run as "Input" samples. The remaining 80% of total protein was used for the pull-down assay and incubated with biotinylated peptides or Klotho antibody. "Output" samples were generated after pull-down by beads as described in panel A. The bar graph depicts the quantification of protein pull-down (n = 2). (C) Pull-down of Klotho by K18-Biotin can be competed off by unlabeled K18 in a dose-dependent manner, but not by K3A up to 200 nM. The bar graph depicts protein quantification in the competition pull-down assay (n = 2). (D) Silver stain analysis was performed on the eluents

https://doi.org/10.1021/jacsau.3c00650
JACS Au 2024, 4, 1334−1344

Figure 4. continued

to investigate the selectivity of pull-down. The lanes corresponding to K18-Biotin and Klotho antibody were the only conditions in which Klotho was enriched significantly. Pep-10-Biotin and K3A-Biotin both were not able to enrich Klotho at 200 nM. Other protein pull-down bands were similar across all lanes, which indicated selective pull-down of Klotho over other proteins by K18-Biotin and Klotho antibody. The bar graph depicts protein quantification in the silver stain normalized to vehicle (n = 2). (E) Pull-down probe K18-Biotin enriched endogenous hKlotho from human kidney lysate but not liver lysate at 50 nM. Negative-control probe K3A-Biotin displayed no enrichment of Klotho from kidney lysate at 50 nM. The bar graph depicts the quantification of protein pull-down from human tissue lysates (n = 2). *P < 0.05, **P < 0.01, ***P < 0.001, as determined by student's t test. Error bars indicate SD.

binding assays. Since K18 was derived from Pep-10 which was originally developed from the binding domain of FGF23,[13] competition binding assays were performed to confirm affinity matured K18 still binds to the same binding site of FGF23. Binding affinity of FGF23 to hKlotho was 151 nM as measured by BLI (Figure S13). K18 and K3A were assessed in the competition binding assays with BLI, and competition K_Ds were determined as 9.8 nM for K18 and over 10 μM for K3A (Figure S13). Competing off FGF23 binding to hKlotho by K18 but not K3A demonstrated that K18 binds Klotho at the same site as FGF23. With all the validations above, K18 was therefore carried forward to downstream target engagement assays.

2.4. Pull-Down Assays Demonstrate Direct Klotho Engagement by K18

We investigated K18's engagement with Klotho in a complex cellular environment using human kidney 2 (HK-2), a proximal tubular cell line that expresses detectable levels of Klotho.[25] In an immunoprecipitation assay, K18-Biotin was incubated with HK-2 cell lysate and pulled down by streptavidin magnetic beads. K18-Biotin-bound proteins were released and separated by gel electrophoresis (Figure 4A). Klotho was significantly enriched in the pulled-down fraction by K18-Biotin starting at 10 nM, consistent with its K_D determined by BLI (Figure 4B). The negative-control probe K3A-Biotin had no enrichment at 50 nM, and precursor peptide Pep-10-Biotin displayed minor enrichment of Klotho at 2 μM (Figure 4B). We also performed a control pull-down using a readily accessible Klotho antibody (KM2076) to verify that the protein enriched from lysate was indeed Klotho.[26] Bands with the same molecular weight were produced in the pull-down fraction by K18-Biotin and Klotho antibodies (Figure 4B), further ensuring the identity of the enriched protein as Klotho.

In a self-competition assay, unlabeled K18 added to the HK-2 cell lysate can compete off the pull-down of Klotho by K18-Biotin in a dose-dependent manner but not by K3A at the same doses (Figure 4C). The results of direct and self-competition pull-down assays showed direct Klotho engagement by K18 in HK-2 cell lysate. Silver stain was performed on the eluents to investigate the selectivity of pull-down by K18-Biotin from HK-2 cell lysate. Using 50 nM of biotinylated peptides, Klotho was the only significantly enriched protein by K18-Biotin and the Klotho antibody but was not enriched by Pep-10-Biotin, K3A-Biotin or vehicle (Figure 4D). To further confirm the observed 130 kDa band is Klotho, the same silver stain was performed using lysate from a different cell line with low Klotho expression, CaSki cells.[14,27] No 130 kDa band was pulled down by K18-Biotin or the Klotho antibody from CaSki cell lysate, confirming that this band is Klotho (Figure S14). These results demonstrated the potential of K18-Biotin to selectively capture Klotho from cell lysate.

Given the ability of K18-Biotin to enrich Klotho in a complex biological mixture, we further evaluated Klotho engagement in human tissue lysate (Figure S15). Klotho has a high level of expression in the kidney but not in the liver. K18-Biotin at 50 nM enriched Klotho from human kidney lysate but not from the liver lysate (Figure 4E). K3A-Biotin at 50 nM had no significant pull-down, even from kidney lysate (Figure 4E). These studies demonstrated the direct engagement of K18 to endogenous total hKlotho in both kidney cell lysate and human tissue lysate, supporting the potential of this peptide-based affinity reagent to engage its target protein in the biological milieu selectively.

2.5. K18-TAMRA Labels Klotho in Cells

Reliable and selective peptide probes to label Klotho in cells are lacking. Due to K18's high affinity and selectivity to recognize Klotho in cell lysate, we used K18-derived fluorescent affinity reagent K18-TAMRA for fluorescence microscopy imaging in HK-2 cells. Live HK-2 cells were grown to 70% confluence, treated with fluorescent peptides, washed, and fixed. The cell membrane in these assays was demarcated with the membrane-specific dye Wheat Germ Agglutinin (WGA) Alexa Fluor 350 Conjugate. After 5 min of incubation, a strong fluorescence signal was obtained upon incubation with 50 nM of K18-TAMRA (Figure 5A). K3A-TAMRA was also tested at the same conditions but did not display appreciable fluorescence emission, suggesting its minimal binding to Klotho in cells (Figure S16). To validate that the fluorescence of K18-TAMRA came primarily from labeling Klotho instead of nonspecific staining inside cells, we performed target engagement and competition studies using recombinant hKlotho and unlabeled K18. K18-TAMRA's fluorescence emission signal was significantly weaker after being preincubated with 500 nM of recombinant hKlotho, consistent with less free unbound K18-TAMRA available for cell uptake and labeling (Figure 5A,B). K18-TAMRA's fluorescence emission signal was also considerably decreased after pretreatment of cells with 500 nM of unlabeled K18 due to the competition of available Klotho binding sites between unlabeled K18 and K18-TAMRA (Figure 5A,B).

To further validate that K18-TAMRA's fluorescent labeling depends on Klotho protein level, we knocked down ∼50% of the endogenous Klotho levels in HK-2 cells using siRNAs (KL siRNA).[14] Afterward, treatment with K18-TAMRA showed reduced fluorescence in HK-2 cells (Figure S17). Meanwhile, mock transfection had no effect on fluorescence, as expected (Figure S17). In CaSki cells with low Klotho expression,[14,27] K18-TAMRA was incubated using a similar protocol to HK-2 cells. K18-TAMRA displayed a significantly lower fluorescence intensity in CaSki cells relative to that of Klotho-expressing HK-2 cells (Figure S18). These results support the Klotho-dependent fluorescent labeling by K18-TAMRA, indicating K18-TAMRA's engagement with Klotho in cells.

https://doi.org/10.1021/jacsau.3c00650
JACS Au 2024, 4, 1334−1344

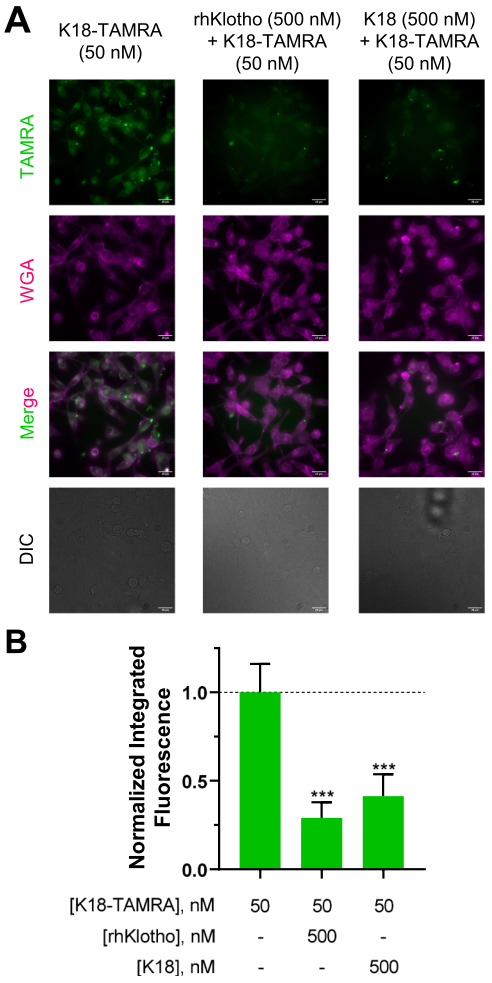

Figure 5. Fluorescence microscopy imaging reveals target engagement of K18-TAMRA labeling total Klotho in HK-2 cells. (A) Left: detection of intracellular fluorescence and potential labeling of endogenous total hKlotho following 5 min of cotreatment with K18-TAMRA at 50 nM and Wheat Germ Agglutinin (WGA) Alexa Fluor 350 Conjugate at 25 ng/μL. Fixation of cells was performed after the treatment. Fluorescence of K18-TAMRA was acquired in the orange channel ($\lambda_{ex/em}$ = 542/597 nm). Fluorescence of WGA Alexa Fluor 350 was acquired in the blue channel ($\lambda_{ex/em}$ = 390/435 nm). Middle: HK-2 cells treated for 5 min with a mixture of preincubated K18-TAMRA (50 nM) and recombinant hKlotho (rhKlotho, 500 nM) displayed significantly decreased intracellular fluorescence. Right: HK-2 cells were pretreated with K18 (50 nM) for 1 h, followed by cotreatment of K18-TAMRA at 50 nM and WGA at 25 ng/μL. The pretreatment of K18 also displayed significantly decreased intracellular fluorescence. (B) Bar graph depicts the quantification of normalized integrated fluorescence of TAMRA in panel A using ImageJ (n = 10 cells from 2 separate cell dishes). ***P < 0.001, as determined by student's t test. Error bars indicate SD. Scale bar = 25 μm.

Since K18-TAMRA selectively labels Klotho in cells endogenously expressing Klotho, we compared the fluorescence microscopy images of K18-TAMRA with the Klotho antibody (KM2076). Despite the slow overnight labeling of the Klotho antibody, its fluorescence patterns were similar to K18-TAMRA (Figure S19). These findings support Klotho's cytoplasmic and membrane location, consistent with the reported results and our previous findings.[14,28] Notably, the current widely used Klotho antibody KM2076 is not suited for live cell labeling since it requires overnight incubation, additional permeation procedures, and hours of incubation with the secondary antibody, which are detrimental to live cells.[26] The fluorescent peptide K18-TAMRA, however, could be used with live HK-2 cells due to a short incubation time (5 min) and mild conditions (Figure S20). These imaging studies demonstrated that K18-TAMRA is a suitable and selective probe for the fluorescent labeling of Klotho in cells.

We expected to observe both intracellular and transmembrane Klotho levels by fluorescence imaging experiments. Cells were detached during culture using trypsin-EDTA, however, which may cleave the linker between the KL1 and KL2 domains of transmembrane Klotho (PDB: 5W21) during cell detachment. Our peptides do not bind to Klotho postdomain cleavage since they mimic the C-terminus of FGF23, the native epitope binding the KL1 and KL2 domains simultaneously. The Klotho antibody (KM2076) also does not bind to Klotho after cleavage, since it recognizes a sequence within the KL1 domain. We hypothesize that at the time of the imaging experiments, the majority of newly produced full-length Klotho proteins were located intracellularly and did not reach the cell membrane and that the majority of the peptide amount had been internalized, leading to preferential detection of Klotho inside the cells.

3. CONCLUSIONS

Peptides can recognize undruggable proteins due to their ability to mimic the proteins' native binding epitopes and capture features of molecular interactions.[29−31] Compared to protein-binding biomacromolecules, peptides have several advantages, including a lower molecular weight (<10 kDa), better stability in complex biological media, and possible cell barrier-penetrating properties. Peptides are also synthetically accessible for large-scale manufacture by solid-phase synthesis and are easily diversifiable by introducing unnatural amino acids. Furthermore, peptides generally show enhanced specificity and lower off-target rates compared to small molecules, making them a promising avenue for therapeutic development.[32]

In this study, high-affinity peptides were discovered using AS-MS as reagents and probes to engage Klotho in a complex cellular context. Multiple biophysical and biochemical assays were employed to validate the enhanced binding affinities of these peptides, which were found to be at least 2300-fold higher. Additionally, these peptides were developed as fluorescent labeling reagents for live cell imaging.

While more research is necessary to fully characterize the potential of these affinity reagents in vivo, these Klotho-recognizing peptides hold promise as potential diagnostic tools for patients with CKD and other aging-related diseases. The significant medicinal and market potential of peptide-based therapeutics is expected to continue to attract funding and scientific attention in the near- and long-term future.

4. METHODS

4.1. Cell Culture

All cells were cultured at 37 °C in 5% CO_2. CaSki cells (ATCC, CRL-1550) were cultured in RPMI 1640 medium (ATCC, 30-2001) supplemented with 1 Pen Strep solution (Gibco, 15140-122) and 10% fetal bovine serum (Sigma, 12003C). HK-2 cells (ATCC, CRL-2190) were cultured in Keratinocyte SFM (Gibco, 17005042) supplemented with bovine pituitary extract and human recombinant EGF.

https://doi.org/10.1021/jacsau.3c00650
JACS Au 2024, 4, 1334−1344

4.2. Pull-Down Assay

HK-2 cells were washed with 1× PBS and harvested by scraping. Total protein was extracted using RIPA lysis buffer (Millipore, 20-188) supplemented with 1× cOmplete Protease Inhibitor Cocktail (Sigma-Aldrich, catalog no. CO-RO) according to the manufacturer's instructions. The cell lysate (200 μg) was then incubated for 30 min at room temperature with K18-Biotin or K3A-Biotin. Unlabeled peptides were preincubated in the cell lysate for 15 min before the addition of biotinylated probes for the competitive pull-down assay. After incubation, 20 μL of streptavidin magnetic beads (Dynabeads MyOne Streptavidin T1, Invitrogen, 65601) were added to the solution to pull-down Klotho, and samples were shaken at room temperature for 20 min. 1× PBS was used to wash the samples. Each sample's proteins were eluted from the beads with incubation with 30 μL of 8 M urea solution at room temperature for 30 min, then resolved on a sodium dodecyl sulfate (SDS)-polyacrylamide gel (Bolt 4−12% Bis-Tris Plus, Invitrogen, NW04120BOX), followed by protein transfer to a nitrocellulose (0.45 μm) membrane. After blocking the membrane in 1× TBST containing 5% (w/v) nonfat milk for 1 h, it was incubated at 4 °C overnight with 1× TBST containing 5% milk and Klotho (Cosmo Bio, KM2076) primary antibody (1:1000 dilution). The membrane was washed three times with 1× TBST for 10 min before being incubated for 1 h with an anti-rat IgG horseradish-peroxidase-linked antibody (Cell Signaling Technology, 7077S) in 1× TBST containing 5% milk. For 15 min, the membrane was washed three times with 1× TBST. The SuperSignal West Pico PLUS Chemiluminescent Substrate was then used to detect Klotho (Thermo Scientific, 34580). The protein bands were quantified using ImageJ software. "Input" or "Output" western blots were performed on protein samples before or after pull-down. Before pull-down, 20% of total protein from the cell lysate protein sample was prepared and run as "Input" samples. The remaining 80% of total protein was used for the pull-down assay and incubated with biotinylated peptides or Klotho antibody. "Output" samples were generated after pull-down by beads as described in Figure 4A. Following the separation of pull-down samples on SDS-polyacrylamide gel according to the manufacturer's protocol, silver staining was performed (Pierce Silver Stain Kit, Thermo Scientific, 24612).

4.3. Cell Imaging

In a 35 mm dish, HK-2 cells were seeded and grown to 70% confluency. The cells were washed with 1× PBS after the medium was removed. Klotho in cells was labeled with peptides by incubating them in 1 mL of HBSS media (Gibco, 24020-117) containing 50 nM of K18-TAMRA or K3A-TAMRA and 25 ng/μL of WGA Alexa FluorTM 350 Conjugate for 5 min at 37 °C. Following incubation, the cells were washed three times with 1× PBS before being fixed in 400 μL of 4% paraformaldehyde (Thermo Scientific) at room temperature for 30 min. After fixation, the cells were washed three times with 1× PBS before imaging. Klotho in cells was labeled with antibody after being fixed in 400 μL of 4% paraformaldehyde (Thermo Scientific) for 30 min and permeabilized in 400 μL of 0.1% Triton X-100 (Sigma-Aldrich, T8787) for 10 min at room temperature. The cells were washed with 1× PBS three times before being blocked for 1 h at room temperature with 2% BSA (w/v) in 1× PBS. The cells were then incubated overnight at 4 °C with Klotho (Cosmo Bio, KM2076) primary antibody (1:250 dilution) in 0.1% BSA. The primary antibody was removed, and the cells were washed three times with 1× PBS. After washing, the cells were incubated in the dark for 1 h with anti-rat IgG Alexa Fluor 647 Conjugate (Cell Signaling Technology, 4418S) in 0.1% BSA. The cells were then washed three times with 1× PBS before imaging.

Images were taken using a DeltaVision Ultra microscope equipped with a scientific Complementary Metal−Oxide−Semiconductor (sCMOS) camera. A xenon arc lamp and a solid-state illumination (InsightSSI) module were used as the light source. The acquisition of images of a given culture dish was performed at a constant transmission and exposure time for each channel. TAMRA was imaged at the orange channel ($\lambda_{ex/em}$ = 542/597 nm) with transmission of 50% and exposure time of 0.2 s. WGA was imaged at the blue channel ($\lambda_{ex/em}$ = 390/435 nm) with transmission of 50% and exposure time of 0.1 s. Antibody was imaged at the red channel ($\lambda_{ex/em}$ = 632/679 nm) with transmission of 20% and exposure time of 0.2 s. The Acquire Ultra software was used to operate the microscope. The ImageJ software (version 2.9.0) was used to calculate the intensity of intracellular fluorescence. The entire cell body was chosen as the region of interest for each measurement. The integrated fluorescence intensity of the cell body region was subtracted from the integrated fluorescence intensity of the background region.

4.4. Transfection in HK-2 Cells

KL siRNA (SMARTpool: ON-TARGETplus Human KL siRNA) was purchased from Horizon Discovery Ltd. (catalog number L-011936-01-0005). The KL siRNA was transfected into cells using the Lipofectamine RNAiMAX reagent (Invitrogen) according to the manufacturer's protocol to a final concentration of 0.1 μM. HK-2 cells were seeded in a 35 mm dish and grown to a 50% confluency. After that, 7.5 μL of RNAiMAX reagent was diluted in 125 μL of the Opti-MEM medium. Similarly, KL siRNA was diluted in 125 μL of the Opti-MEM medium. Diluted siRNA was mixed with diluted RNAiMAX reagent and incubated at room temperature for 5 min. The total 250 μL solution was added to a 35 mm dish and incubated at 37 °C for 2 days before treatment with peptides of interest or western blot. Mock-transfected cells were those that were added to a solution containing only the RNAiMAX reagent.

■ ASSOCIATED CONTENT

Data Availability Statement

The data supporting the findings of this study are available in the main text and in the Supporting Information.

Supporting Information

The Supporting Information is available free of charge at https://pubs.acs.org/doi/10.1021/jacsau.3c00650.

Detailed methods and materials, and LC−MS characterization of peptides (PDF)

■ AUTHOR INFORMATION

Corresponding Authors

Magdalena Preciado López − *Calico Life Sciences LLC, South San Francisco, California 94080, United States*; Email: magdalena@calicolabs.com

Bradley L. Pentelute − *Department of Chemistry and Center for Environmental Health Sciences, Massachusetts Institute of Technology, Cambridge, Massachusetts 02139, United States; The Koch Institute for Integrative Cancer Research, Massachusetts Institute of Technology, Cambridge, Massachusetts 02142, United States; Broad Institute of MIT and Harvard, Cambridge, Massachusetts 02142, United States*; orcid.org/0000-0002-7242-801X; Email: blp@mit.edu

Authors

Peiyuan Zhang − *Department of Chemistry, Massachusetts Institute of Technology, Cambridge, Massachusetts 02139, United States*

Xiyun Ye − *Department of Chemistry, Massachusetts Institute of Technology, Cambridge, Massachusetts 02139, United States*; Present Address: Department of Chemistry, Graduate School of Science, The University of Tokyo, 7-3-1, Hongo, Bunkyo, Tokyo 113-0033, Japan (X.Y.)

John C. K. Wang − *Calico Life Sciences LLC, South San Francisco, California 94080, United States*

Corey L. Smith − *AbbVie Bioresearch Center, Worcester, Massachusetts 01605, United States*

Silvino Sousa − *AbbVie Bioresearch Center, Worcester, Massachusetts 01605, United States*
Andrei Loas − *Department of Chemistry, Massachusetts Institute of Technology, Cambridge, Massachusetts 02139, United States;* orcid.org/0000-0001-5640-1645
Dan L. Eaton − *Calico Life Sciences LLC, South San Francisco, California 94080, United States*

Complete contact information is available at: https://pubs.acs.org/10.1021/jacsau.3c00650

Author Contributions

P.Z., X.Y., M.P.L., and B.L.P. conceived the project; P.Z. and X.Y. performed experiments with input from A.L., D.L.E., M.P.L., and B.L.P.; J.C.K.W., C.L.S., and S.S. generated Klotho protein; P.Z. and X.Y. generated figures and wrote the manuscript with input from all authors; P.Z. and X.Y. contributed equally to this work. CRediT: **Peiyuan Zhang** conceptualization, data curation, formal analysis, investigation, methodology, writing-original draft, writing-review & editing; **Xiyun Ye** conceptualization, data curation, investigation, methodology, validation, writing-original draft, writing-review & editing; **John C. K. Wang** data curation, investigation, project administration, resources, software, validation; **Corey L. Smith** data curation, investigation, methodology; **Silvino Sousa** data curation, investigation, methodology; **Andrei Loas** data curation, formal analysis, project administration, supervision, writing-review & editing; **Dan L. Eaton** conceptualization, formal analysis, funding acquisition, project administration, resources; **Magdalena Preciado López** conceptualization, data curation, formal analysis, funding acquisition, project administration, resources, supervision, writing-review & editing; **Bradley L. Pentelute** conceptualization, data curation, formal analysis, funding acquisition, supervision, writing-review & editing.

Notes

The authors declare the following competing financial interest(s): B.L.P. is a co-founder and/or member of the scientific advisory board of several companies focusing on the development of protein and peptide therapeutics.

■ ACKNOWLEDGMENTS

The financial support for this work was provided by Calico Life Sciences LLC (to B.L.P.). We acknowledge support from the Swanson Biotechnology Center Microscopy Core Facility at the Koch Institute for Integrative Cancer Research at MIT through the use of their epifluorescence microscope (NCI Cancer Center Support Grant P30-CA14051).

■ REFERENCES

(1) Kuro-o, M.; Matsumura, Y.; Aizawa, H.; Kawaguchi, H.; Suga, T.; Utsugi, T.; Ohyama, Y.; Kurabayashi, M.; Kaname, T.; Kume, E.; Iwasaki, H.; Iida, A.; Shiraki-Iida, T.; Nishikawa, S.; Nagai, R.; Nabeshima, Y. I. Mutation of the mouse klotho gene leads to a syndrome resembling ageing. *Nature* **1997**, *390* (6655), 45−51.
(2) Iijima, H.; Gilmer, G.; Wang, K.; Bean, A. C.; He, Y.; Lin, H.; Tang, W. Y.; Lamont, D.; Tai, C.; Ito, A.; Jones, J. J.; Evans, C.; Ambrosio, F. Age-related matrix stiffening epigenetically regulates alpha-Klotho expression and compromises chondrocyte integrity. *Nat. Commun.* **2023**, *14* (1), 18.
(3) Lim, K.; Groen, A.; Molostvov, G.; Lu, T.; Lilley, K. S.; Snead, D.; James, S.; Wilkinson, I. B.; Ting, S.; Hsiao, L. L.; Hiemstra, T. F.; Zehnder, D. alpha-Klotho Expression in Human Tissues. *J. Clin Endocrinol Metab* **2015**, *100* (10), E1308−E1318.
(4) Chen, G.; Liu, Y.; Goetz, R.; Fu, L.; Jayaraman, S.; Hu, M. C.; Moe, O. W.; Liang, G.; Li, X.; Mohammadi, M. alpha-Klotho is a non-enzymatic molecular scaffold for FGF23 hormone signalling. *Nature* **2018**, *553* (7689), 461−466.
(5) Kuro, O. M. The Klotho proteins in health and disease. *Nat. Rev. Nephrol.* **2019**, *15* (1), 27−44.
(6) Kim, J. H.; Hwang, K. H.; Park, K. S.; Kong, I. D.; Cha, S. K. Biological Role of Anti-aging Protein Klotho. *J. Lifestyle Med.* **2015**, *5* (1), 1−6.
(7) Neyra, J. A.; Hu, M. C. Potential application of klotho in human chronic kidney disease. *Bone* **2017**, *100*, 41−49.
(8) Zhou, L.; Li, Y.; Zhou, D.; Tan, R. J.; Liu, Y. Loss of Klotho contributes to kidney injury by derepression of Wnt/beta-catenin signaling. *J. Am. Soc. Nephrol* **2013**, *24* (5), 771−785.
(9) Laszczyk, A. M.; Fox-Quick, S.; Vo, H. T.; Nettles, D.; Pugh, P. C.; Overstreet-Wadiche, L.; King, G. D. Klotho regulates postnatal neurogenesis and protects against age-related spatial memory loss. *Neurobiol Aging* **2017**, *59*, 41−54.
(10) Castner, S. A.; Gupta, S.; Wang, D.; Moreno, A. J.; Park, C.; Chen, C.; Poon, Y.; Groen, A.; Greenberg, K.; David, N.; Boone, T.; Baxter, M. G.; Williams, G. V.; Dubal, D. B. Longevity factor klotho enhances cognition in aged nonhuman primates. *Nat. Aging* **2023**, *3*, 931−937.
(11) Doi, S.; Zou, Y.; Togao, O.; Pastor, J. V.; John, G. B.; Wang, L.; Shiizaki, K.; Gotschall, R.; Schiavi, S.; Yorioka, N.; Takahashi, M.; Boothman, D. A.; Kuro, O. M. Klotho inhibits transforming growth factor-beta1 (TGF-beta1) signaling and suppresses renal fibrosis and cancer metastasis in mice. *J. Biol. Chem.* **2011**, *286* (10), 8655−8665.
(12) Valeur, E.; Gueret, S. M.; Adihou, H.; Gopalakrishnan, R.; Lemurell, M.; Waldmann, H.; Grossmann, T. N.; Plowright, A. T. New Modalities for Challenging Targets in Drug Discovery. *Angew. Chem., Int. Ed. Engl.* **2017**, *56* (35), 10294−10323.
(13) Agrawal, A.; Ni, P.; Agoro, R.; White, K. E.; DiMarchi, R. D. Identification of a second Klotho interaction site in the C terminus of FGF23. *Cell Rep* **2021**, *34* (4), No. 108665.
(14) Ye, X.; Zhang, P.; Wang, J. C. K.; Smith, C. L.; Sousa, S.; Loas, A.; Eaton, D. L.; Preciado Lopez, M.; Pentelute, B. L. Branched Multimeric Peptides as Affinity Reagents for the Detection of alpha-Klotho Protein. *Angew. Chem., Int. Ed. Engl.* **2023**, *62*, No. e202300289.
(15) Touti, F.; Gates, Z. P.; Bandyopadhyay, A.; Lautrette, G.; Pentelute, B. L. In-solution enrichment identifies peptide inhibitors of protein-protein interactions. *Nat. Chem. Biol.* **2019**, *15* (4), 410−418.
(16) Ye, X.; Lee, Y. C.; Gates, Z. P.; Ling, Y.; Mortensen, J. C.; Yang, F. S.; Lin, Y. S.; Pentelute, B. L. Binary combinatorial scanning reveals potent poly-alanine-substituted inhibitors of protein-protein interactions. *Commun. Chem.* **2022**, *5* (1), 128.
(17) Torner, J. M.; Yang, Y.; Rooklin, D.; Zhang, Y.; Arora, P. S. Identification of Secondary Binding Sites on Protein Surfaces for Rational Elaboration of Synthetic Protein Mimics. *ACS Chem. Biol.* **2021**, *16* (7), 1179−1183.
(18) Frank, A. O.; Vangamudi, B.; Feldkamp, M. D.; Souza-Fagundes, E. M.; Luzwick, J. W.; Cortez, D.; Olejniczak, E. T.; Waterson, A. G.; Rossanese, O. W.; Chazin, W. J.; Fesik, S. W. Discovery of a potent stapled helix peptide that binds to the 70N domain of replication protein A. *J. Med. Chem.* **2014**, *57* (6), 2455−2461.
(19) Ye, X.; Zhang, P.; Tao, J.; Wang, J. C. K.; Mafi, A.; Grob, N. M.; Quartararo, A. J.; Baddock, H. T.; Chan, L. J. G.; McAllister, F. E.; Foe, I.; Loas, A.; Eaton, D. L.; Hao, Q.; Nile, A. H.; Pentelute, B. L. Discovery of reactive peptide inhibitors of human papillomavirus oncoprotein E6. *Chemical Science* **2023**, *14*, 12484−12497.
(20) Gesmundo, N. J.; Sauvagnat, B.; Curran, P. J.; Richards, M. P.; Andrews, C. L.; Dandliker, P. J.; Cernak, T. Nanoscale synthesis and affinity ranking. *Nature* **2018**, *557* (7704), 228−232.
(21) Quartararo, A. J.; Gates, Z. P.; Somsen, B. A.; Hartrampf, N.; Ye, X.; Shimada, A.; Kajihara, Y.; Ottmann, C.; Pentelute, B. L. Ultra-large chemical libraries for the discovery of high-affinity peptide binders. *Nat. Commun.* **2020**, *11* (1), 3183.

(22) Gates, Z. P.; Vinogradov, A. A.; Quartararo, A. J.; Bandyopadhyay, A.; Choo, Z. N.; Evans, E. D.; Halloran, K. H.; Mijalis, A. J.; Mong, S. K.; Simon, M. D.; Standley, E. A.; Styduhar, E. D.; Tasker, S. Z.; Touti, F.; Weber, J. M.; Wilson, J. L.; Jamison, T. F.; Pentelute, B. L. Xenoprotein engineering via synthetic libraries. *Proc. Natl. Acad. Sci. U. S. A.* **2018**, *115* (23), E5298−E5306.
(23) Dikler, S.; Kelly, J. W.; Russell, D. H. Improving mass spectrometric sequencing of arginine-containing peptides by derivatization with acetylacetone. *J. Mass Spectrom* **1997**, *32* (12), 1337−1349.
(24) Altschul, S. F.; Madden, T. L.; Schaffer, A. A.; Zhang, J.; Zhang, Z.; Miller, W.; Lipman, D. J. Gapped BLAST and PSI-BLAST: a new generation of protein database search programs. *Nucleic Acids Res.* **1997**, *25* (17), 3389−3402.
(25) Guan, X.; Nie, L.; He, T.; Yang, K.; Xiao, T.; Wang, S.; Huang, Y.; Zhang, J.; Wang, J.; Sharma, K.; Liu, Y.; Zhao, J. Klotho suppresses renal tubulo-interstitial fibrosis by controlling basic fibroblast growth factor-2 signalling. *J. Pathol* **2014**, *234* (4), 560−572.
(26) Kato, Y.; Arakawa, E.; Kinoshita, S.; Shirai, A.; Furuya, A.; Yamano, K.; Nakamura, K.; Iida, A.; Anazawa, H.; Koh, N.; Iwano, A.; Imura, A.; Fujimori, T.; Kuro-o, M.; Hanai, N.; Takeshige, K.; Nabeshima, Y. Establishment of the anti-Klotho monoclonal antibodies and detection of Klotho protein in kidneys. *Biochem. Biophys. Res. Commun.* **2000**, *267* (2), 597−602.
(27) Lee, J.; Jeong, D. J.; Kim, J.; Lee, S.; Park, J. H.; Chang, B.; Jung, S. I.; Yi, L.; Han, Y.; Yang, Y.; Kim, K. I.; Lim, J. S.; Yang, I.; Jeon, S.; Bae, D. H.; Kim, C. J.; Lee, M. S. The anti-aging gene KLOTHO is a novel target for epigenetic silencing in human cervical carcinoma. *Mol. Cancer* **2010**, *9*, 109.
(28) Xu, Y.; Sun, Z. Molecular basis of Klotho: from gene to function in aging. *Endocr Rev.* **2015**, *36* (2), 174−193.
(29) Hillig, R. C.; Sautier, B.; Schroeder, J.; Moosmayer, D.; Hilpmann, A.; Stegmann, C. M.; Werbeck, N. D.; Briem, H.; Boemer, U.; Weiske, J.; Badock, V.; Mastouri, J.; Petersen, K.; Siemeister, G.; Kahmann, J. D.; Wegener, D.; Bohnke, N.; Eis, K.; Graham, K.; Wortmann, L.; von Nussbaum, F.; Bader, B. Discovery of potent SOS1 inhibitors that block RAS activation via disruption of the RAS-SOS1 interaction. *Proc. Natl. Acad. Sci. U. S. A.* **2019**, *116* (7), 2551−2560.
(30) Grossmann, T. N.; Yeh, J. T.; Bowman, B. R.; Chu, Q.; Moellering, R. E.; Verdine, G. L. Inhibition of oncogenic Wnt signaling through direct targeting of beta-catenin. *Proc. Natl. Acad. Sci. U. S. A.* **2012**, *109* (44), 17942−17947.
(31) Bird, G. H.; Mazzola, E.; Opoku-Nsiah, K.; Lammert, M. A.; Godes, M.; Neuberg, D. S.; Walensky, L. D. Biophysical determinants for cellular uptake of hydrocarbon-stapled peptide helices. *Nat. Chem. Biol.* **2016**, *12* (10), 845−852.
(32) Muttenthaler, M.; King, G. F.; Adams, D. J.; Alewood, P. F. Trends in peptide drug discovery. *Nat. Rev. Drug Discov* **2021**, *20* (4), 309−325.

https://doi.org/10.1021/jacsau.3c00650
JACS Au 2024, 4, 1334−1344